

# NOVEL NON-LOCAL TOTAL VARIATION REGULARIZATION FOR CONSTRAINED MR RECONSTRUCTION

Andres Saucedo<sup>1,2</sup>, Stamatis Lefkimiatis<sup>3</sup>, Stanley Osher<sup>3</sup>, and Kyunghyun Sung<sup>1,2</sup>

<sup>1</sup>Department of Radiological Sciences, David Geffen School of Medicine, University of California Los Angeles, Los Angeles, California, United States, <sup>2</sup>Biomedical Physics Interdepartmental Graduate Program, University of California Los Angeles, Los Angeles, California, United States, <sup>3</sup>Department of Mathematics, University of California Los Angeles, Los Angeles, California, United States

**Target Audience:** MR researchers in reconstruction and clinicians for fast imaging

**Purpose:** Compressed Sensing (CS) and Parallel Imaging (PI) methods accelerate acquisition speed by significantly reducing k-space sampling yet produce high quality images by imposing *a priori* and data-based information as constraints. Recently, constrained reconstruction has made extensive use of low-rank models, including in the calibrationless PI approaches [1,2], which enforce a global low-rankness of multi-coil data in k-space, or a local low-rankness across multiple coils in the image domain. In this work, we introduce a novel image domain-based constrained reconstruction technique, applicable for CS & PI, that exploits the correlation of the image data across different coils and the inherent non-local self-similarity property of images (image structures tend to repeat themselves in an image scene) using a non-local total variation (NLTV) regularization framework.

**Theory:** Non-local regularization techniques capture information about complex image structures [3] and favor reconstructions that exhibit the non-local self-similarity property. In this work, we employ the NLTV regularizer [3] in a novel setting and obtain image reconstructions from multiple MRI acquisitions without the explicit knowledge of the coil sensitivities. Our image reconstruction is formulated as the solution of the following optimization problem:

$$x^* = \arg \min_{\mathbf{x} \in \mathbb{C}^N} 0.5 \|\mathbf{y} - \mathbf{Ex}\|_2^2 + \tau \left( \sum_{c=1}^C \|\nabla_{NL} \mathbf{x}_c\|^2 \right)^{1/2}$$

where  $\mathbf{E}$  is the multi-coil encoding operator,  $\mathbf{y}$  is k-space data,  $\mathbf{x}_c$  is the  $c$ -th underlying coil image, and  $\nabla_{NL}$  is the non-local graph gradient. The minimizer is obtained by utilizing the Split-Bregman method [4]. The final image corresponds to the sum-of-squares (SoS) of the  $\mathbf{C}$  estimates.

**Methods:** NLTV was applied to reconstruct a  $256 \times 256$  image matrix of an 8-channel multi-coil brain image data retrospectively undersampled with random, variable density sampling masks at reduction factors (RF) 2 – 7. These images were normalized with respect to maximum image magnitude, and contaminated with 5 levels of Gaussian noise (standard deviations  $\sigma = 0.01, 0.02, 0.03, 0.04, \& 0.05$  corresponding to maximum SNR's of 100, 50, 33, 25, & 20, respectively). All k-space data contained a fully sampled  $20 \times 20$  central region. For comparison purposes, CLEAR [1] was also applied to the same data set. Both the NLTV and CLEAR algorithms were implemented in MATLAB (version 8.1) and run on a Linux workstation with a 4.4 GHz CPU and 96 GB memory. The thresholding parameter for CLEAR adaptively adjusts in proportion to the median magnitude of transform-domain coefficients, whereas the regularization parameter for NLTV was optimized empirically by minimizing the normalized root-mean square error (nRMSE) for all cases. The patch size for CLEAR was set to  $8 \times 8$ , and the number of non-local weights, the patch size and search window for NLTV were set to 9,  $7 \times 7$ , and  $11 \times 11$ , respectively. Each algorithm was run for a maximum of 60 iterations. For all cases, the zero-filled sum-of-squares (SoS) image was pre-smoothed and used to estimate the non-local weights

necessary in the definition of the NLTV penalty. For the computation of the distance between image patches the Euclidean norm of their difference was used (Fig.1). The nRMSE values of the SoS images, computation times, and visual assessment of image quality serve as the basis for comparison.

**Results:** For SNR's below approximately 67, and for all reduction factors, NLTV has superior performance in terms of nRMSE and image quality, as compared to CLEAR (Table 1). As seen in Fig. 2, NLTV is able to minimize contribution from noise, yet preserves fine features without the oversmoothing typical of local TV. NLTV's reconstruction time is significantly faster at  $305 \pm 86$  seconds (s), while that of CLEAR is  $626 \pm 71$  s.

**Discussion:** NLTV shows competitive results in relation to other image domain-based constrained methods that incorporate a local smoothness prior in the reconstruction. However, results indicate that NLTV has similar or slightly less accuracy under cases of very low or no-added noise (Fig.3). Nonetheless, even as the reduction factor and noise level increases, NLTV reconstruction exhibits great stability in terms of nRMSE. At a given reduction factor, the nRMSE increases only by approximately 0.01 from lowest to highest noise, whereas CLEAR, for example, produces results that increase by up to 0.025.

**Conclusion:** The proposed method encompasses a joint CS-PI approach by exploiting data redundancy using multiple coils to achieve high-quality reconstruction. NLTV-based regularization demonstrates substantial advantages with regard to high levels of noise. This type of reconstruction may better serve applications that suffer from inherent SNR limitations.

**References:** [1] Trzasko, J.D., Manduca, A. (Asilomar Conf., IEEE, 2011) [2] Shin et. al., MRM (2013) [3] Gilboa, G., Osher, S., SIAM (2008) [4] Goldstein T., Osher, S., SIAM (2009)

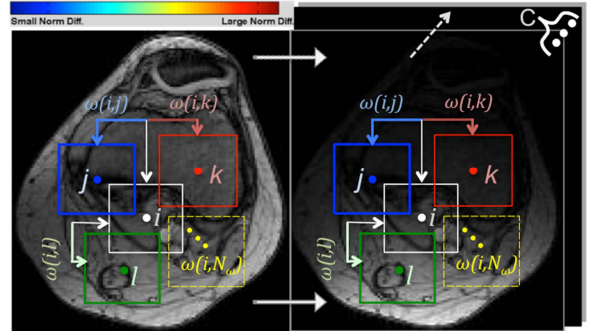


**Fig. 1:** Illustration of weights computation for pixel  $i$  (centered in white patch), estimated with a pre-smoothed zero-filled SoS image (left), then enforced along all  $C$  coil images (right).

Noise \ RF	2	3	4	5	6	7
0	0.037/0.026	0.046/0.036	0.051/0.043	0.054/0.049	0.055/0.054	0.058/0.057
0.01	0.038/0.028	0.047/0.038	0.051/0.045	0.053/0.049	0.055/0.053	0.058/0.056
0.02	0.041/0.04	0.048/0.049	0.053/0.054	0.055/0.058	0.056/0.06	0.059/0.063
0.03	0.044/0.05	0.051/0.058	0.055/0.063	0.056/0.065	0.058/0.067	0.06/0.07
0.04	0.048/0.06	0.053/0.067	0.057/0.071	0.058/0.073	0.06/0.074	0.062/0.077
0.05	0.051/0.07	0.056/0.075	0.059/0.078	0.06/0.08	0.061/0.081	0.064/0.083

**Table 1:** nRMSE values (NLTV/CLEAR) for various levels of noise and reduction factors

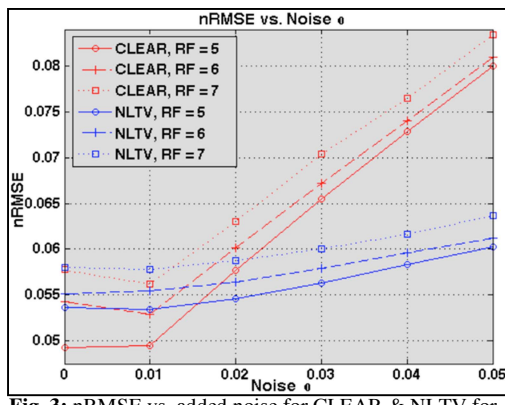


**Fig. 3:** nRMSE vs. added noise for CLEAR & NLTV for reduction factors 5, 6, & 7.

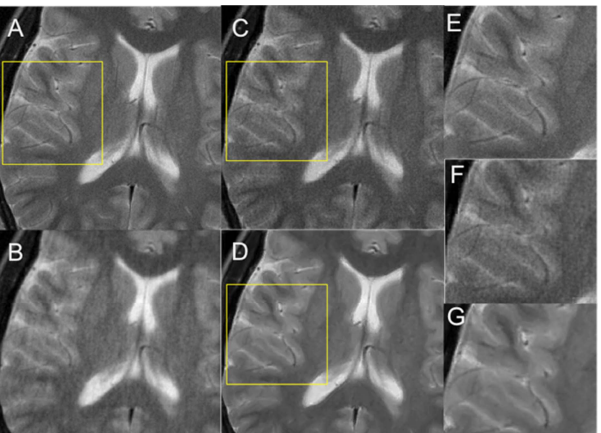


**Fig. 2:** Reconstructed image results for reduction factor 5 and  $\sigma = 0.03$ . (A) Fully-sampled original (B) Zero-filled (C) CLEAR (D) NLTV (E) Zoom-in of original (F) Zoom-in of CLEAR (G) Zoom-in of NLTV